Three-Band Biorthogonal Interpolating Complex Wavelets with Stopband Suppression via Lifting Scheme

Peng-Lang Shui, *Member, IEEE*, Zheng Bao, *Senior Member, IEEE*, and Yuan Yan Tang, *Senior Member, IEEE*

***Abstract*—Recent wavelet research has primarily focused on real-valued wavelet bases. However, the complex filterbanks provide much convenience for complex signal processing. For example, in radar and sonar signal processing, the complex signals from the I/Q receiver can be efficiently processed with complex filterbanks rather than real filterbanks. Specifically, the positive and negative Doppler frequencies imply different physical content in the moving target detector (MTD) and moving target identification (MTI); therefore, it is significant to design complex multiband filterbanks that can partition positive and negative frequencies into different subbands. In the paper, we design two novel families of three-band biothogonal interpolating complex filterbanks and wavelets by using the three-band lifting scheme. Unlike the traditional three-band filterbanks, the novel complex filterbank is composed of three channels, including the lowpass channel, the positive highpass channel whose passband distributes in the positive frequency region, and the negative highpass channel in the negative frequency region. Such a filterbank/wavelet naturally provides the ability to extract positive frequency components and negative frequency components from complex signals. Moreover, a novel set of design constraints are introduced to manipulate the stopband characteristic of highpass filters and are referred to as the stopband suppression, which strengthens the traditional constraints of vanishing moments. Finally, a numerical method is given to further lower stopband sidelobes.**

***Index Terms*—Biorthogonal interpolating complex wavelets, stopband suppression, three-band lifting scheme.**

I. Introduction

OVER the last two decades, various methodologies have been developed to construct real wavelets in the mathematical analysis and in the signal processing literature. These methodologies provide abundant real wavelets, including various types of two-band wavelets, M-band wavelets, and multiwavelets [1]–[8], from which appropriate wavelets can be selected to apply to special applications. When real signals are processed, real filterbanks and wavelets are a natural choice for their symmetric amplitude frequency responses, which just match the symmetric power spectrums of real signals. However, complex signals usually have asymmetric power spectrums. A typical case is analytic signals that only contain positive frequency content. In this case, real wavelets and filterbanks are no longer an efficient tool since the real and imaginary parts have to be processed separately. Moreover, for some special applications, complex wavelets are still desired to provide special characteristics that real wavelets cannot provide. For example, in radar and sonar signal processing, signals from the I/Q receiver are complex, and specifically, the positive and negative Doppler frequencies imply different physical content in the moving target detector (MTD) and moving target identification (MTI) [9], [10]; therefore, it is significant to design complex multiband filterbanks that can partition the positive and negative frequencies into different subbands. In fact, in the time-frequency analysis, the complex-valued bases have been widely used to represent complex signals, such as the short-time Fourier transform (STFT), the Gabor transform, and the "Chirplet" transform [11]–[14]. Their common advantage is that the positive frequency components and negative frequency components can be separately extracted.

Recently, complex-valued filterbanks and wavelets have been attracting much attention [15]–[26]. The research mainly focuses on the two-band complex wavelets. By allowing the complex filter's coefficients, two-band complex wavelets can simultaneously possess compact support, symmetry/antisymmetry, and orthogonality [15]–[17], which is impossible for two-band real filterbanks and wavelets. Complex filters with symmetry or antisymmetry retain symmetric amplitude frequency responses and thus cannot partition the positive and negative frequency components in different subbands. Relaxation of symmetry allows us to obtain two-band complex filterbanks with asymmetric amplitude frequency responses [16]; however, the asymmetry is not enough to partition the positive and negative frequency components into different subbands. The Gabor-like complex filterbanks [20] and modulated complex filterbanks [21] possess the ability but are without the perfect reconstruction. Selesnick [23], [24] designed pairs of two-band wavelets where two wavelets form an approximate Hilbert transform pair. Such a pair of wavelets can effectively separate the positive and negative frequency components from complex signals. Kingsbury and Fernandes [22], [25], [26] devised two-dimensional (2-D) directional complex wavelets with redundancy. These 2-D complex wavelets are provided with the shift-invariance and directional selectivity that the traditional 2-D real wavelets cannot achieve.

In the paper, we design two novel families of three-band biorthogonal interpolating complex filterbanks and wavelets

Manuscript received September 14, 2001; revised November 19, 2002. This work was supported by the Foundation for Author of National Excellent Doctoral Dissertation of P.R. China under Project 200139. The associate editor coordinating the review of this paper and approving it for publication was Dr. Masaaki Ikehara.

P.-L. Shui and Z. Bao are with the Key Laboratory for Radar Signal Processing, Xidian University, Xi'an, China (e-mail: plshui@xidian.edu.cn).

Y. Y. Tang is with the Department Computer Science, Hong Kong Baptist University, Hong Kong.

Digital Object Identifier 10.1109/TSP.2003.810282

by using the three-band lifting scheme. Unlike the traditional three-band filterbanks, such a filterbank has three channels:

1) the lowpass channel;
2) the positive highpass channel whose passband distributes in the positive frequency region;
3) the negative highpass channel in the negative frequency region.

Thus, the filterbank and the associated wavelet naturally provide the ability to extract positive and negative frequency components from complex signals.

The lifting scheme is a flexible framework to construct biorthogonal filterbanks developed recently by Sweldens [27]–[29]. The early works in [30], [31] were related with the lifting scheme. Later, the lifting scheme was extended to the multidimensional and M-channel case [32]. The lifting scheme completely absorbs the biorthogonal constraints into the filterbank's structure itself. Thus, starting from a simple filterbank (e.g., "Lazy" wavelet), one can design various filterbanks and wavelets by selection of lifting filters. Therein, the lifting filters are either real-valued or complex-valued. Due to this flexibility, the lifting idea has been widely utilized in many applications, such as the adaptive subband coding and image compression [33]–[35].

In this paper, we first review the three-band lifting scheme and establish the two structures of three-band biorthogonal interpolating filterbanks with three pairs of lifting filters. In the first structure, the interpolating scaling filters are real, but the dual scaling filters must be complex. The second structure compensates this deficiency and allows both the interpolating scaling filter and the dual scaling filter to be real-valued. In Section III, the novel set of design constraints, namely, the stopband suppression, are introduced, which strengthen the traditional constraints of vanishing moments. Then, two important theorems are proved, which present a sufficient and necessary condition on moments of lifting filters for the complex filterbanks to be $(K+1)$-regular and of $(K+1)$ order stopband suppression. In Section IV, two families of regular biorthogonal interpolating complex filterbanks and wavelets are devised. First, we design interpolating complex filterbanks with symmetric interpolating scaling filters with minimal length, and these filterbanks have explicit solutions but suffer from high stopband sidelobes. Therefore, we give up the demand of minimal length and use part of degrees of freedom to lower the stopband sidelobes by a numerical method. The method improves the stopband attenuation of filters but only obtains the numerical solutions of filters.

Throughout this paper, $H(z)$ and $H(\omega)$ denote the z-transform and frequency response of a filter $h(n)$, respectively. Let $T(z)=\sum t(n)z^{-n}$ be a z-polynomial; then, $\overline{T}(z)$ represents the z-polynomial $\sum \overline{t(n)}z^{-n}$, where $\overline{t(n)}$ is the conjugate of a complex number $t(n)$; let $\mathbf{H}(z)=[H_{ij}(z)]$ be a polyphase matrix; then, $\mathbf{H}^{\dagger}(z)=[\overline{H}_{ij}(z)]'$, where the superscript $'$ represents the transposition of a matrix. $C_k^p=k!/p!(k-p)!$.

II. Three-Band Lifting Scheme

The lifting scheme is a flexible framework to construct biorthogonal filterbanks, which was proposed by Sweldens [27], [28] in 1995. The early works in [30] and [31] were related to the lifting scheme as well. In the two-band lifting scheme, each step updates one subband decomposition coefficients using another subband coefficients, and two steps consist of a total lifting procedure, which have been widely used to construct two-band biorthogonal filterbanks. Later, the lifting scheme was extended to the multidimensional and M-band $(M>2)$ case and was used to construct multidimensional biorthogonal filterbanks. Unlike the two-band lifting scheme, the M-band lifting scheme includes multifarious patterns. In what follows, we will present two patterns of the three-band lifting scheme.

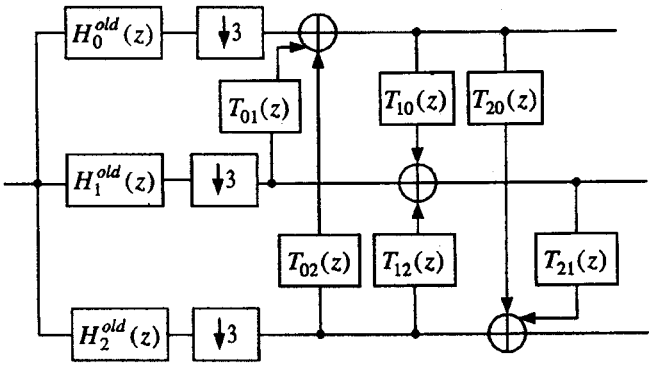

Fig. 1. Flow diagram of type I three-band lifting scheme.

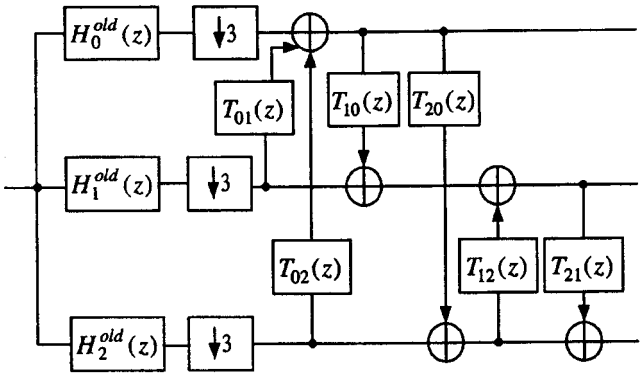

Fig. 2. Flow diagram of type II three-band lifting scheme.

The two-band lifting scheme can be easily extended to the M-band case $(M\geq 3)$ and multidimensional case [32]. Here, we only consider the three-band lifting scheme. The type I three-band lifting scheme is divided into three simple steps, and in each step, one channel is updated with help of the other two channels, as shown in Fig. 1. The type I is a direct extension of the two-band lifting scheme. Operating the type I on the three-band "Lazy wavelet," we obtain a family of three-band biorthogonal interpolating complex filterbanks, and such filterbanks have real interpolating scaling filters but complex dual scaling filters. Therefore, the type II three-band lifting scheme is proposed as illustrated in Fig. 2. It compensates the deficiency of the type I and allows both the interpolating scaling filter and the dual scaling filter to be real-valued, which will be described in the next section.

Definition 1: Let $\{h_i^{\mathrm{old}}, i=0,1,2\}$ and $\{g_i^{\mathrm{old}}, i=0,1,2\}$ be a three-band FIR biorthogonal filterbank and $\mathbf{H}_{\mathrm{old}}(z)$ and $\mathbf{G}_{\mathrm{old}}(z)$ be their polyphase matrices; then, the

type I three-band lifting scheme is defined with polyphase representation as follows:

$$\begin{aligned}\mathbf{H}_{\text{new}}(z) &= \mathbf{T}_2(z)\mathbf{T}_1(z)\mathbf{T}_0(z)\mathbf{H}_{\text{old}}(z)\\ \mathbf{G}_{\text{new}}(z) &= \mathbf{S}_2(z^{-1})\mathbf{S}_1(z^{-1})\mathbf{S}_0(z^{-1})\mathbf{G}_{\text{old}}(z)\end{aligned} \tag{1}$$

where

$$\mathbf{T}_0(z) = \begin{bmatrix} 1 & T_{01}(z) & T_{02}(z) \\ 0 & 1 & 0 \\ 0 & 0 & 1 \end{bmatrix}$$

$$\mathbf{T}_1(z) = \begin{bmatrix} 1 & 0 & 0 \\ T_{10}(z) & 1 & T_{12}(z) \\ 0 & 0 & 1 \end{bmatrix}$$

$$\mathbf{T}_2(z) = \begin{bmatrix} 1 & 0 & 0 \\ 0 & 1 & 0 \\ T_{20}(z) & T_{21}(z) & 1 \end{bmatrix}$$

$$\mathbf{S}_i(z) = 2\mathbf{I}_3 - \mathbf{T}_i^{\dagger}(z), \qquad i = 0,\ 1 \text{ and } 2.$$

Similarly, the type II three-band lifting scheme is defined as follows:

$$\begin{aligned}\mathbf{H}_{\text{new}}(z) &= \mathbf{T}_3(z)\mathbf{T}_2(z)\mathbf{T}_1(z)\mathbf{T}_0(z)\mathbf{H}_{\text{old}}(z)\\ \mathbf{G}_{\text{new}}(z) &= \mathbf{S}_3(z^{-1})\mathbf{S}_2(z^{-1})\mathbf{S}_1(z^{-1})\mathbf{S}_0(z^{-1})\mathbf{G}_{\text{old}}(z)\end{aligned} \tag{2}$$

where $\mathbf{T}_0(z)$ is identical to that in the type I, and

$$\mathbf{T}_1(z) = \begin{bmatrix} 1 & 0 & 0 \\ T_{10}(z) & 1 & 0 \\ T_{20}(z) & 0 & 1 \end{bmatrix}$$

$$\mathbf{T}_2(z) = \begin{bmatrix} 1 & 0 & 0 \\ 0 & 1 & T_{12}(z) \\ 0 & 0 & 1 \end{bmatrix}$$

$$\mathbf{T}_3(z) = \begin{bmatrix} 1 & 0 & 0 \\ 0 & 1 & 0 \\ 0 & T_{21}(z) & 1 \end{bmatrix}$$

$$\mathbf{S}_i(z) = 2\mathbf{I}_3 - \mathbf{T}_i^{\dagger}(z), \qquad i = 0,\ 1,\ 2 \text{ and } 3$$

where $T_{i,j}(e^{j\omega})$ are real or complex trigonometric polynomials.

From the above definition, six lifting filters completely determine three-band lifting procedures. For the type I lifting scheme, each channel is updated with help of a pair of lifting filters in turn. From

$$\mathbf{G}_{\text{new}}^{\dagger}(z^{-1})\mathbf{H}_{\text{new}}(z) = \mathbf{G}_{\text{old}}^{\dagger}(z^{-1})\prod_{i=0}^{2}\mathbf{S}_i^{\dagger}(z)\prod_{i=2}^{0}\mathbf{T}_i(z)\mathbf{H}_{\text{old}}(z)$$

and $\mathbf{S}_i^{\dagger}(z)\,\mathbf{T}_i(z) = \mathbf{I}_3$ for $i = 0,\ 1,\ 2$, we have

$$\mathbf{G}_{\text{new}}^{\dagger}(z^{-1})\mathbf{H}_{\text{new}}(z) = \mathbf{G}_{\text{old}}^{\dagger}(z^{-1})\mathbf{H}_{\text{old}}(z) = \mathbf{I}_3. \tag{3}$$

Therefore, the new filterbank is biorthogonal. Similarly, the filterbanks generated by the type II lifting scheme are biorthogonal as well; this way, one can freely select six lifting filters (either real or complex), whereas these do not influence on the biorthogonality. Moreover, from (1) and (2), six new filters in the type I have the z-transforms, shown in (4) and (5) at the bottom of the page.

Six new filters in the type II have the z-transforms as follows:

$$\begin{aligned}H_0^{\text{new}}(z) &= H_0^{\text{old}}(z) + T_{01}(z^3)H_1^{\text{old}}(z) + T_{02}(z^3)H_2^{\text{old}}(z)\\ H_1(z) &= H_1^{\text{old}}(z) + T_{10}(z^3)H_0(z)\\ H_2(z) &= H_2^{\text{old}}(z) + T_{20}(z^3)H_0(z)\\ H_1^{\text{new}}(z) &= H_1(z) + T_{12}(z^3)H_2(z)\\ H_2^{\text{new}}(z) &= H_2(z) + T_{21}(z^3)H_1^{\text{new}}(z)\end{aligned} \tag{6}$$

$$\begin{aligned}G_1(z) &= G_0^{\text{old}}(z) - \overline{T}_{01}(z^{-3})\\ G_2(z) &= G_2^{\text{old}}(z) - \overline{T}_{02}(z^{-3})\\ G_0^{\text{new}}(z) &= 1 - \overline{T}_{10}(z^{-3})G_1(z) - \overline{T}_{20}(z^{-3})G_2(z)\\ G_2^{\text{new}}(z) &= G_2(z) - \overline{T}_{12}(z^{-3})G_1(z)\\ G_1^{\text{new}}(z) &= G_1(z) - \overline{T}_{21}(z^{-3})G_2^{\text{new}}(z).\end{aligned} \tag{7}$$

Like the two-band lifting scheme, the above two three-band lifting patterns provide an efficient approach to construct three-band biorthogonal filterbanks and wavelets. Besides the above two patterns, one can also consider other patterns of the three-band lifting scheme.

III. Biorthogonal Interpolating Complex Filterbanks With Stopband Suppression

In continuous-time signal processing, one must consider the initialization of wavelet transform that converts continuous-time signals into discrete-time signals. The conversion usually results in the initialization error. In order to reduce or remove the error, except for the prefiltering techniques, the interpolating wavelets are a simple and efficient approach. A filter in an M-band filterbank is called the cardinal interpolating

$$\begin{bmatrix} H_0^{\text{new}}(z) \\ H_1^{\text{new}}(z) \\ H_2^{\text{new}}(z) \end{bmatrix} == \begin{bmatrix} H_0^{\text{old}}(z) + T_{01}(z^3)H_1^{\text{old}}(z) + T_{02}(z^3)H_2^{\text{old}}(z) \\ T_{10}(z^3)H_0^{\text{new}}(z) + H_1^{\text{old}}(z) + T_{12}(z^3)H_2^{\text{old}}(z) \\ T_{20}(z^3)H_0^{\text{new}}(z) + T_{21}(z^3)H_1^{\text{new}}(z) + H_2^{\text{old}}(z) \end{bmatrix} \tag{4}$$

$$\begin{bmatrix} G_0^{\text{new}}(z) \\ G_1^{\text{new}}(z) \\ G_2^{\text{new}}(z) \end{bmatrix} = \begin{bmatrix} \left[1 + \overline{T}_{10}(z^{-3})\overline{T}_{01}(z^{-3})\right] G_0^{\text{old}}(z) - \overline{T}_{10}(z^{-3})G_1^{\text{old}}(z) - \overline{T}_{20}(z^{-3})G_2^{\text{new}}(z) \\ G_1^{\text{old}}(z) - \overline{T}_{01}(z^{-3})G_0^{\text{old}}(z) - \overline{T}_{21}(z^{-3})G_2^{\text{new}}(z) \\ G_2^{\text{old}}(z) - \left[\overline{T}_{02}(z^{-3}) - \overline{T}_{12}(z^{-3})\overline{T}_{01}(z^{-3})\right] G_0^{\text{old}}(z) - \overline{T}_{12}(z^{-3})G_1^{\text{old}}(z) \end{bmatrix} \tag{5}$$

filter if it satisfies $h(Mn) = \delta(n)$. Similarly, a scaling function $\psi_0(x)$ in an M-band wavelet is the cardinal interpolating scaling function if it satisfies $\psi_0(n) = \delta(n)$ [36]–[38]. In this case, the associated wavelet is referred to as an interpolating wavelet. In the two-band case, by operating the lifting scheme on the "Lazy wavelet" [27], [37], the biorthogonal interpolating real wavelets were constructed.

Typically, a three-band "Lazy wavelet" is

$$\begin{bmatrix} H_0^{Lazy}(z) \\ H_1^{Lazy}(z) \\ H_2^{Lazy}(z) \end{bmatrix} = \begin{bmatrix} G_0^{Lazy}(z) \\ G_1^{Lazy}(z) \\ G_2^{Lazy}(z) \end{bmatrix} = \begin{bmatrix} 1 \\ z^{-1} \\ z^{-2} \end{bmatrix}. \tag{8}$$

When the type I lifting scheme operates on the "Lazy wavelet," we obtain a family of biorthogonal interpolating filterbanks represented by (9) and (10), shown at the bottom of the page. When the type II lifting scheme operates on the "Lazy wavelet," we obtain another family of biorthogonal interpolating filterbanks by (11) and (12), also shown at the bottom of the page.

Obviously, $h_0(3n) = \delta(n)$, and H_0 is a cardinal interpolating filter. Notice that the filters H_0, G_2, and G_1 in the type II are identical with those in the type I, whereas G_0, H_1, and H_2 are different from those in the type I. After the filterbanks are obtained, the associated scaling functions and wavelets can be derived from the following two-scale difference equations:

$$\begin{aligned}
\psi_0(x) &= \sum_n h_0(n)\psi_0(3x-n),\ \tilde{\psi}_0(x) = \sum_n g_0(n)\tilde{\psi}_0(3x-n) \\
\psi_1(x) &= \sum_n h_1(n)\psi_0(3x-n),\ \tilde{\psi}_0(x) = \sum_n g_1(n)\tilde{\psi}_0(3x-n) \\
\psi_2(x) &= \sum_n h_2(n)\psi_0(3x-n),\ \tilde{\psi}_0(x) = \sum_n g_2(n)\tilde{\psi}_0(3x-n).
\end{aligned}$$

A. Design Constraints of Stopband Suppression

Complex signals usually have asymmetric power spectrums with respect to the zero frequency, and a typical case is analytic signals that only contain positive frequency content. When complex signals are processed, complex filterbanks and wavelets provide more advantages than their real counterparts. In this case, the real and imaginary parts of signals can been processed jointly rather than separately, and thus, the inherent relationship between real and imaginary parts can be sufficiently utilized. Moreover, in special applications, complex wavelets are desired to provide special characteristics that real wavelets cannot provide. For example, in radar and sonar signal processing, signals from the I/Q receiver are complex, and the positive and negative Doppler frequencies have different physical content in the moving target detector and identification (MTD and MTI) [9], [10]; therefore, we desire multiband complex filterbanks and wavelets that can partition the positive and negative frequencies into different subbands/channels. In the time-frequency analysis, most continuous-type transforms such as the short-time Fourier transform (STFT), the Gabor transform, and the "Chirplet" transform [11]–[14] possess the ability. Recent research on complex filterbanks and wavelets mainly focuses on compatibility of compact support, orthogonality, and symmetry/antisymmetry [15]–[17]. In some applications, multiband complex filterbanks or pairs of two-band filterbanks have provided this ability [20], [21], [23], [24]. Therefore, we want the three-band complex filterbanks to have the amplitude frequency responses, as shown in Fig. 3 in the ideal case. In Fig. 3, H_0 is the lowpass channel with the passband $[-(\pi/3), \pi/3]$, H_1 is the positive highpass channel with the passband $[\pi/3, \pi]$, and H_2 is the negative highpass channel with the passband $[-\pi, -(\pi/3)]$. Moreover, when a three-band complex wavelet is provided with the above frequency segmentation, the associated tree-structural wavelet

$$\begin{bmatrix} H_0(z) \\ H_1(z) \\ H_2(z) \end{bmatrix} = \begin{bmatrix} 1 + z^{-1}T_{01}(z^3) + z^{-2}T_{02}(z^3) \\ z^{-1} + T_{10}(z^3)H_0(z) + z^{-2}T_{12}(z^3) \\ z^{-2} + T_{20}(z^3)H_0(z) + T_{21}(z^3)H_1(z) \end{bmatrix} \tag{9}$$

$$\begin{bmatrix} G_0(z) \\ G_1(z) \\ G_2(z) \end{bmatrix} = \begin{bmatrix} \left[1 + \overline{T}_{10}(z^{-3})\overline{T}_{01}(z^{-3})\right] - z^{-1}\overline{T}_{10}(z^{-3}) - \overline{T}_{20}(z^{-3})G_2(z) \\ z^{-1} - \overline{T}_{01}(z^{-3}) - \overline{T}_{21}(z^{-3})G_2(z) \\ z^{-2} - \left[\overline{T}_{02}(z^{-3}) - \overline{T}_{12}(z^{-3})\overline{T}_{01}(z^{-3})\right] - z^{-1}\overline{T}_{12}(z^{-3}) \end{bmatrix} \tag{10}$$

$$\begin{bmatrix} H_0(z) \\ H_1(z) \\ H_2(z) \end{bmatrix} = \begin{bmatrix} 1 + z^{-1}T_{01}(z^3) + z^{-2}T_{02}(z^3) \\ z^{-1} + [T_{10}(z^3) + T_{12}(z^3)T_{20}(z^3)]H_0(z) + z^{-2}T_{12}(z^3) \\ z^{-2} + T_{20}(z^3)H_0(z) + T_{21}(z^3)H_1(z) \end{bmatrix} \tag{11}$$

$$\begin{bmatrix} G_0(z) \\ G_1(z) \\ G_2(z) \end{bmatrix} = \begin{bmatrix} \left[1 + \overline{T}_{01}(z^{-3})\overline{T}_{10}(z^{-3}) + \overline{T}_{02}(z^{-3})\overline{T}_{20}(z^{-3})\right] - z^{-1}\overline{T}_{10}(z^{-3}) - z^{-2}\overline{T}_{20}(z^{-3}) \\ z^{-1} - \overline{T}_{01}(z^{-3}) - \overline{T}_{21}(z^{-3})G_2(z) \\ z^{-2} - \left[\overline{T}_{02}(z^{-3}) - \overline{T}_{12}(z^{-3})\overline{T}_{01}(z^{-3})\right] - z^{-1}\overline{T}_{12}(z^{-3}) \end{bmatrix} \tag{12}$$

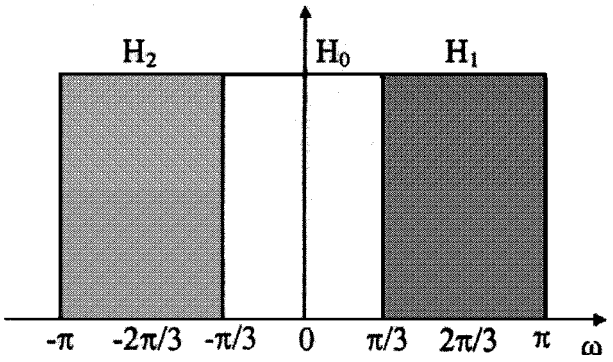

Fig. 3. Three-band ideal complex wavelet.

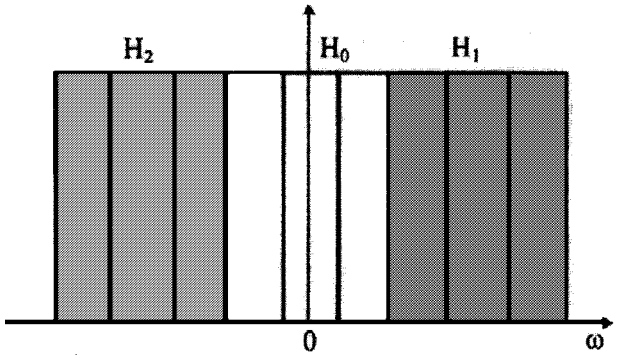

Fig. 4. Two-level three-band ideal complex packet.

packet [39] provides a finer frequency segmentation, for example, the two-level ideal three-band complex wavelet packet, as shown in Fig. 4.

However, FIR filterbanks cannot achieve the ideal frequency responses as in Fig. 3, and thus, we want their amplitude frequency responses to approximate the ideal case. In order to realize this intention, we introduce a novel set of design constraints, namely, stopband suppression. The traditional wavelet design uses the regularity order and vanishing moments [1], [7] to handle the passband and stopband of a filter. In the two-band case, the regularity order manipulates the passband flatness and stopband attenuation of a scaling filter as well as the approximation power of the associated multiresolution analysis, and vanishing moments manipulate the stopband attenuation of highpass filter. However, in the M-band case ($M > 2$), the vanishing moments of bandpass and highpass filters only manipulate the attenuation around $\omega = 0$ rather than the total stopband.

A $(K + 1)$-regular three-band scaling filter $H_0(z)$ satisfies [7]

$$H_0^{(k)}\left(\frac{2\pi}{3}\right) = H_0^{(k)}\left(-\frac{2\pi}{3}\right) = 0, \qquad k = 0, 1, \ldots, K \tag{13}$$

where $H_0^{(k)}(\omega)$ denotes the kth-order derivative with respect to ω. $H_0(\omega)$ has two $(K+1)$-degree zero points $\pm(2\pi/3)$, which manipulate its stopband attenuation. A wavelet filter $h_i(n)$ has $(K + 1)$ vanishing moments if $\sum_n n^k h_i(n) = 0$, for $k = 0, 1, \ldots, K$, which only indicates $H_i(\omega)$ has one $(K + 1)$-degree zero point $\omega = 0$, and thus, vanishing moments only manipulate its attenuation around $\omega = 0$.

In Fig. 3, three filters have the centers of the passbands $\omega = 0$, $(2/3)\pi$, and $-(2/3)\pi$, respectively. For a three-band FIR complex filterbank, the $(K+1)$-order regularity of the lowpass filter H_0 suppresses the positive and negative high-frequency components in the lowpass channel owing to two $(K + 1)$-degree zero points $\omega = \pm(2/3)\pi$. Similarly, in the two highpass channels H_1 and H_2, we impose two pairs of $(K + 1)$-degree zero points on $\omega = 0$, $-(2/3)\pi$, and $\omega = 0$, $(2/3)\pi$, respectively. These two pairs of zero points suppress low frequency and negative high-frequency components in the channel H_1 and low-frequency and positive high-frequency components in the channel H_2, respectively. Therefore, we introduce the novel set of design constraints, namely, the stopband suppression, to manipulate the stopband characteristics of H_1 and H_2.

Definition 2: In a three-band complex filterbank, the highpass filters H_1 and H_2 have the $(K+1)$-order stopband suppression if the frequency responses satisfy: For $k = 0, 1, \ldots, K$

$$\begin{aligned} H_1^{(k)}(0) &= H_1^{(k)}\left(-\tfrac{2}{3}\pi\right) = 0 \\ H_2^{(k)}(0) &= H_2^{(k)}\left(\tfrac{2}{3}\pi\right) = 0 \end{aligned} \tag{14}$$

and $H_1((2/3)\pi) \neq 0$, $H_2(-(2/3)\pi) \neq 0$.

Obviously, the $(K+1)$-order stopband suppression is stricter than the $(K + 1)$-order vanishing moments for H_1 and H_2. Below, we show that the stopband suppression also ensures the passband flatness of highpass filters.

B. Biorthogonal Interpolating Complex Filterbanks With Stopband Suppression

For the type I filterbanks given in (9) and (10) and the type II filterbanks given in (11) and (12), the two main theorems are proved. The two theorems give a sufficient and necessary condition for filterbank $\{H_0, H_1, H_2\}$ to be $(K+1)$-order regular and of $(K + 1)$-order stopband suppression. Moreover, when these conditions are satisfied, the dual filterbank $\{G_0, G_1, G_2\}$ is also $(K + 1)$-order regular and of $(K + 1)$-order stopband suppression. First, we define the moments of lifting filters and present an important lemma.

Lemma 1: Let the lifting filter $T_{il}(z) = \sum_n t_{il}(n)z^{-n}$, and define its k-order moment

$$v_{il}(k) = \sum_n n^k t_{il}(n).$$

Then

$$\begin{aligned} T_{il}^{(k)}(e^{3j\omega})|_{\omega=0,\,\pm(2/3)\pi} &= (-3j)^k v_{il}(k) \\ \overline{T}_{il}^{(k)}(e^{-3j\omega})|_{\omega=0,\,\pm(2/3)\pi} &= (3j)^k \overline{v}_{il}(k). \end{aligned} \tag{15}$$

From $T(e^{3j\omega}) = \sum_n t_{il}(n)e^{-j3n\omega}$, we have

$$T^{(k)}(e^{3j\omega}) = (-3j)^k \sum_n n^k t_{il}(n)e^{-j3n\omega}.$$

Therefore, for $q = 0, \pm 1$

$$\begin{aligned} T^{(k)}(e^{3j\omega})|_{\omega=(2\pi/3)q} &= (-3j)^k \sum_n n^k t_{il}(n)e^{-j2qn\pi} \\ &= (-3j)^k v_{il}(k). \end{aligned}$$

Similarly, the second formula in (15) can be proved.

Theorem 1: For the type I biorthogonal interpolating complex filterbank given in (9), the scaling filter H_0 is $(K+1)$-regular, and the two highpass filters H_1 and H_2 have $(K+1)$-order

stopband suppression if and only if the three pairs of lifting filters satisfy the following: For $k = 0, 1, 2, \ldots, K$

$$\begin{aligned} v_{01}(k) &= \left(-\tfrac{1}{3}\right)^k, \qquad v_{02}(k) = \left(-\tfrac{2}{3}\right)^k \\ v_{10}(k) &= \frac{\alpha^2-1}{3}\left(\frac{1}{3}\right)^k, \qquad v_{12}(k) = -\alpha^2\left(-\frac{1}{3}\right)^k \\ v_{20}(k) &= -\frac{1}{3}\left(\frac{2}{3}\right)^k, \qquad v_{21}(k) = \frac{\alpha}{1-\alpha^2}\left(\frac{1}{3}\right)^k \end{aligned} \tag{16}$$

where $\alpha = e^{j(2/3)\pi}$. Moreover, when (16) is satisfied, the dual scaling filter G_0 is also $(K+1)$-regular, and the highpass filters G_1 and G_2 also have $(K+1)$-order stopband suppression.

The proof of Theorem 1 is given in Appendix A.

From Theorem 1, it is easily observed that when the two highpass filters are $(K+1)$-order stopband suppression, the lifting filters $v_{10}(k)$, $v_{12}(k)$, and $v_{21}(k)$ must be complex, and thus, G_0 must be a complex filter.

Theorem 2: In the type II biorthogonal interpolating complex filterbank given in (11), the scaling filter H_0 is $(K+1)$-regular, and the two highpass filters H_1 and H_2 have $(K+1)$-order stopband suppression if and only if the three pairs of lifting filters satisfy the following: For $k = 0, 1, 2, \ldots, K$

$$\begin{aligned} v_{01}(k) &= \left(-\tfrac{1}{3}\right)^k, \qquad v_{02}(k) = \left(-\tfrac{2}{3}\right)^k \\ v_{10}(k) &= -\tfrac{1}{3}\left(\tfrac{1}{3}\right)^k, \qquad v_{20}(k) = -\tfrac{1}{3}\left(\tfrac{2}{3}\right)^k \\ v_{12}(k) &= -\alpha^2\left(-\frac{1}{3}\right)^k, \quad v_{21}(k) = \frac{\alpha}{1-\alpha^2}\left(\frac{1}{3}\right)^k. \end{aligned} \tag{17}$$

Moreover, when (17) is satisfied, the dual scaling filter G_0 is also $(K+1)$-regular, and the highpass filters G_1 and G_2 also have $(K+1)$-order stopband suppression.

The proof of Theorem 2 is given in Appendix B.

From (12), the lifting filters t_{01}, t_{02}, t_{10}, and t_{20} determine the dual scaling filter G_0. Following the moment conditions (17), G_0 may be a real filter. Utilizing the above results, two families of three-band biorthogonal interpolating complex filterbanks can be designed with arbitrary order regularity and stopband suppression by selecting a set solutions of the linear equations (16) or (17). Moreover, the stopband suppression also ensures the passband flatness of highpass filters.

Corollary 1: For the types I and II filterbanks in Theorems 1 and 2, when the moment conditions (16) and (17) are satisfied, the two scaling filters satisfy the following: For $k = 0, 1, \ldots, K$

$$\begin{aligned} H_0^{(k)}(0) &= 3\delta(k) \\ G_0^{(k)}(0) &= \delta(k) \end{aligned} \tag{18}$$

the four highpass filters are $(K+1)$-order flat around centers of their passbands, that is, for $k = 1, 2, \ldots, K$

$$\begin{aligned} \left.\frac{d^k|H_1(\omega)|^2}{d\omega^k}\right|_{\omega=(2/3)\pi} &= \left.\frac{d^k|G_1(\omega)|^2}{d\omega^k}\right|_{\omega=(2/3)\pi} = 0 \\ \left.\frac{d^k|H_2(\omega)|^2}{d\omega^k}\right|_{\omega=-(2/3)\pi} &= \left.\frac{d^k|G_2(\omega)|^2}{d\omega^k}\right|_{\omega=-(2/3)\pi} = 0. \end{aligned} \tag{19}$$

For the proof, see Appendix C.

Corollary 1 shows that when the moment conditions (16) and (17) are satisfied, all six filters are flat around the centers of their passbands. From the proofs of Theorems 1 and 2, we notice that

$$\begin{aligned} H_0(0) &= 3, \qquad G_0(0) = 1 \\ \left|H_1\left(\tfrac{2}{3}\pi\right)\right| &= \left|G_1\left(\tfrac{2}{3}\pi\right)\right| = |\alpha^2 - 1| = \sqrt{3} \\ \left|H_2\left(-\tfrac{2}{3}\pi\right)\right| &= |\alpha^2| = 1, \qquad \left|G_2\left(-\tfrac{2}{3}\pi\right)\right| = |3\alpha^2| = 3. \end{aligned}$$

For convenience, to compare the magnitude frequency responses of filters, the magnitudes of all filters at their centers of the passbands are made to be consistent and equal to $\sqrt{3}$ by multiplying appropriate factors, in which $H_0(\omega)$ and $G_2(\omega)$ are multiplied by a factor $1/\sqrt{3}$, $G_0(\omega)$, and $H_2(\omega)$ are multiplied by a factor $\sqrt{3}$, whereas $H_1(\omega)$ and $G_1(\omega)$ remain invariant.

IV. Examples

In this section, we first give three-band interpolating complex filterbanks and wavelets with the shortest length. These filterbanks have high stopband sidelobes, and therefore, a numerical method is proposed to lower the stopband sidelobes. By the numerical method, three-band interpolating complex filterbanks and wavelets with low stopband sidelobes are designed.

A. Interpolating Complex Filterbanks and Wavelets With Shortest Length

From the moment conditions (16) and (17), for a three-band interpolating complex filterbank with $(K+1)$-order regularity and stopband suppression, the shortest length of the lifting filters is $K+1$. For a FIR filter $h(n)$, its support set is defined as $\{n \in \mathbf{Z}: \min(S) \le n \le \max(S)\}$, where $S = \{n \in \mathbf{Z}: h(n) \neq 0\}$, and $\mathbf{Z}$ is the integer set. In what follows, we formulize the $(K+1)$-order filterbank with the shortest lifting filters.

The moment conditions (16) and (17) can be rewritten as a unified form

$$\sum_n n^k t_{il}(n) = c_{il}\left(\frac{i-l}{3}\right)^k, \qquad k = 0, 1, \ldots, K \tag{20}$$

where c_{il} is a complex constant given by (16) and (17). It is easy to verify that (20) is equivalent to the following:

$$\sum_n (3n - i + l)^k t_{il}(n) = c_{il}\delta(k), \qquad k = 0, 1, \ldots, K. \tag{21}$$

When the support set of the lifting filter $t_{il}(n)$ is $\{m_{il}, m_{il}+1, \ldots, m_{il}+K\}$, the unique solution of equations is

$$\begin{aligned} t_{il}(n) = c_{il} \prod_{k=m_{il},\, k\neq n}^{m_{il}+K} \frac{3k-i+l}{3(k-n)} \\ n = m_{il}, m_{il}+1, \ldots, m_{il}+K. \end{aligned} \tag{22}$$

The lifting filter in (22) is identical with the three-band *Dubuc* filters, except for a constant factor. As is well-known, the two-band Dubuc filters [40] have been widely used in [27], [28], [35], and [37], which are closely related to the Largrange interpolation.

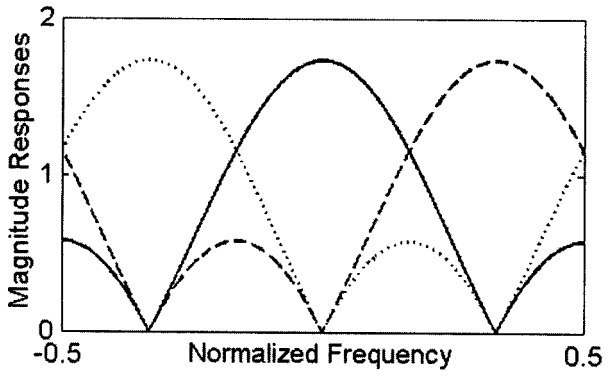

Fig. 5. Magnitude frequency responses of three-band complex Haar wavelet.

When $K = 0$, if we set m_{01}, m_{02}, m_{10}, m_{12}, m_{20} and m_{21} to zero, we obtain a three-band complex filterbank with one order regularity and stopband suppression, and its z-transforms are

$$\begin{aligned} H_0(z) &= (1 + z^{-1} + z^{-2}); \qquad G_0(z) = \tfrac{1}{3} H_0(z) \\ H_1(z) &= G_1(z) = -\frac{\sqrt{3}+j}{2\sqrt{3}} + \frac{\sqrt{3}-j}{2\sqrt{3}}\, z^{-1} + \frac{j}{\sqrt{3}} z^{-2} \\ H_2(z) &= \frac{1}{3}\left(-\frac{1+\sqrt{3}j}{2} + \frac{-1+\sqrt{3}j}{2}\, z^{-1} + z^{-2} \right) \\ G_2(z) &= 3H_2(z). \end{aligned} \tag{23}$$

This is an orthogonal filterbank. Referring to the characteristic of the Haar wavelet, we call it the three-band complex Haar wavelet. Its amplitude frequency responses are illustrated in Fig. 5 (the magnitudes of all filters at their centers of passbands are unified to $\sqrt{3}$ by multiplying appropriate factors).

When $K \geqslant 1$, set

$$m_{il} = \left[-\frac{K}{2} - \frac{l-i}{3} \right] \tag{24}$$

where $[x]$ rounds x to the nearest integer. In this case, the filterbanks provide satisfactory properties.

Proposition 1: When m_{01}, m_{02}, m_{10} and m_{20} satisfy (24), the interpolating scaling filter $H_0(z)$ is a symmetric filter with the shortest length, and the type II the dual scaling filter $G_0(z)$ is also symmetric.

The proof is given in Appendix D.

When K is an odd integer, the length of H_0 is $3K+2$; when K is an even integer, the length is $3K + 3$. The lifting filter $t_{il}(n)$ in (22) is substantially derived from estimating the value of a function at i using its values at $\{3n + l,\ n = m_{il},\ m_{il} + 1, \ldots, m_{il} + K\}$ by the Largrange interpolation. The estimators perform well only when the center of the set $\{3n + l,\ n = m_{il},\ m_{il}+1, \ldots, m_{il}+K\}$ is nearest i, and m_{il}, which is determined by (24), is in accordance with this demand. Therefore, (24) is also used to determine the support sets of the lifting filters $t_{12}(n)$ and $t_{21}(n)$.

In this way, two families of three-band biorthogonal complex filterbanks with the shortest length are designed. The scaling filters $H_0(\omega)$ and $G_0(\omega)$ do not vanish on the $[-(\pi/3),\ \pi/3]$, and thus, the associated complex wavelets are biorthogonal [7]. For example, the type I and type II filterbanks with fourth-order regularity and stopband suppression are illustrated in Figs. 6 and 7.

In Figs. 6 and 7, the magnitudes of all filters at their centers of passbands are unified to the same value $\sqrt{3}$. The left sides are the interpolating filterbanks, and the right sides are the dual filterbanks. Sharp peaks appear between the two adjacent stopband zero points, called the stopband sidelobe. This phenomenon occurs for all filterbanks with the shortest length. High stopband sidelobes degrade the performance of the associated wavelets, and the dual scaling functions have poor smoothness. Following the result in [41], we estimate the Sobolev exponents of the scaling functions and the two types of the dual scaling functions, which are listed in Table I.

B. Complex Filterbanks With Low Stopband Sidelobes

In order to utilize the interpolation, $\{H_0,\ H_1,\ H_2\}$ must be taken as the synthesis filterbank, and thus, $\{G_0,\ G_1,\ G_2\}$ is the analysis filterbank. In many applications, the analysis filterbank is desired to be provided with good frequency selectivity or low stopband sidelobes, which makes the analysis procedure efficiently partition different frequency components into different channels/subbands, whereas the synthesis scaling function is desired to be smooth enough to ensure the smoothness of recovery signals. The smoothness of scaling functions are related with the stopband sidelobe of the scaling filter. Therefore, we develop a numerical method to lower the stopband sidelobes of G_0, G_1, G_2 and H_0.

For the type I and type II filterbanks, we prescribe that the stopband of H_0 and G_0 is $\Omega_0 = [-\pi,\ -(2\pi/3)] \cup [2\pi/3,\ \pi]$, the stopband of H_1 and G_1 is $\Omega_1 = [-(2/3)\pi,\ 0]$, and the stopband of H_2 and G_2 is $\Omega_2 = [0,\ 2\pi/3]$. Since the complex filterbanks with the shortest length suffer from high stopband sidelobes, we relax the demand of the shortest length and use part of the degrees of freedom to lower the stopband sidelobes. Without loss of generality, assume that all lifting filters have length $L+1$ and that the order of regularity and stopband suppression is $K+1$ $(K < L)$; then, $L-K$ degrees of freedom in each lifting filter are used to lower the stopband sidelobes by minimization of the total stopband energy of G_0, G_1, G_2, and H_0. The optimization problem is described as follows:

$$\begin{aligned} \min_{\mathbf{x}} \Bigg\{ & \int_{\Omega_0} \left(\left| \sqrt{3} G_0(\omega) \right|^2 + \left| \frac{1}{\sqrt{3}} H_0(\omega) \right|^2 \right) d\omega \\ & + \int_{\Omega_1} |G_1(\omega)|^2 \, d\omega + \int_{\Omega_2} \left| \frac{1}{\sqrt{3}} G_2(\omega) \right|^2 d\omega \Bigg\} \\ \text{s.t.,} \quad & \sum_{n=mm_{il}}^{mm_{ij}+L} n^k t_{il}(n) = c_{il} \left(-\frac{l-i}{3} \right)^k \\ & \text{for } i,\ l = 0,\ 1,\ 2,\ l \neq i \text{ and } k = 0,\ 1,\ \ldots,\ K \\ & \text{where } \mathbf{x} = [t_{01},\ t_{02},\ t_{10},\ t_{12},\ t_{20},\ t_{21}] \end{aligned} \tag{25}$$

where $mm_{il} = \text{round}(-(L/2) - ((l-i)/2))$, c_{il} are given in (16) or (17). In the objective function, the factors in front of filters make the magnitudes at the centers of their passbands be consistent and equal to $\sqrt{3}$.

The vector $\mathbf{x}$ is composed of six lifting filters. Due to nonlinearity of objective functions, the initial vector is crucial. Here,

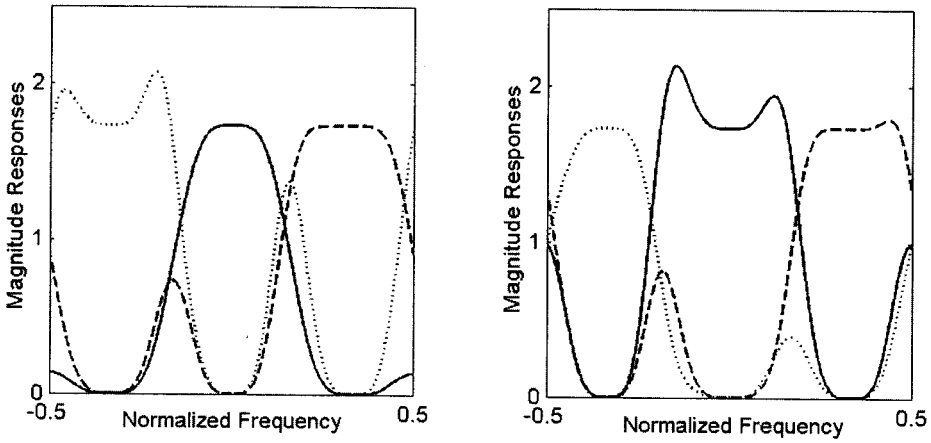

Fig. 6. Type I filterbank with fourth-order regularity and stopband suppression.

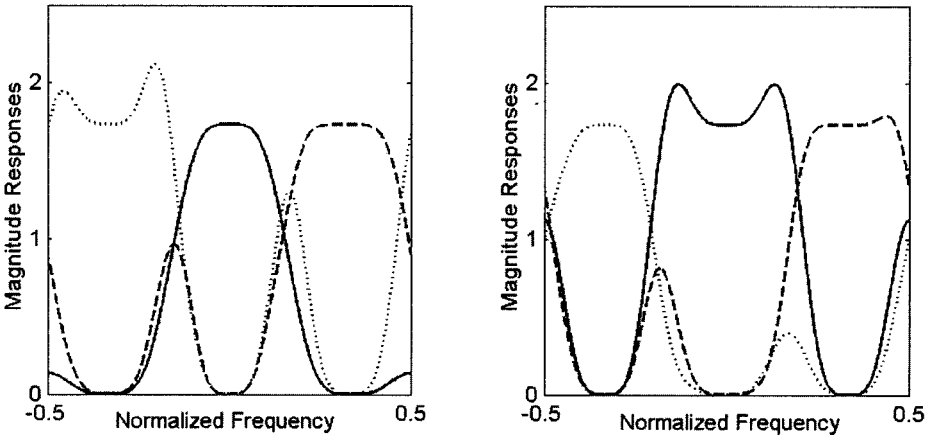

Fig. 7. Type II filterbank with fourth-order regularity and stopband suppression.

TABLE I
SOBOLEV EXPONENTS OF SCALING FUNCTIONS AND DUAL SACLING FUNCTIONS

Regular order	Scaling functions	Dual scaling functions	
K+1	ψ_0	Type I	Type II
2	2.0000	1.0274	0.7105
3	1.9087	0.7105	2.0339
4	2.7105	1.0211	0.8917

the initial vector comes from the $(L+1)$-regular interpolating complex filterbank with the shortest length in Section IV-A. For $L=7$ and $K=4$, the optimized type I filterbank is illustrated in Fig. 8. The associated interpolating scaling function (solid line), the real part (dashed line), and imaginary part (dotted line) of the dual scaling function is depicted in Fig. 9. The interpolating scaling function achieves the Sobolev exponent 2.7489, and the total stopband energy of three analysis filters is 0.1339. For $L=7$ and $K=4$, the optimized type II filterbank is illustrated in Fig. 10. The associated interpolating scaling (solid line) and the dual scaling functions (dashed line) are depicted in Fig. 11. The interpolating scaling function achieves the Sobolev

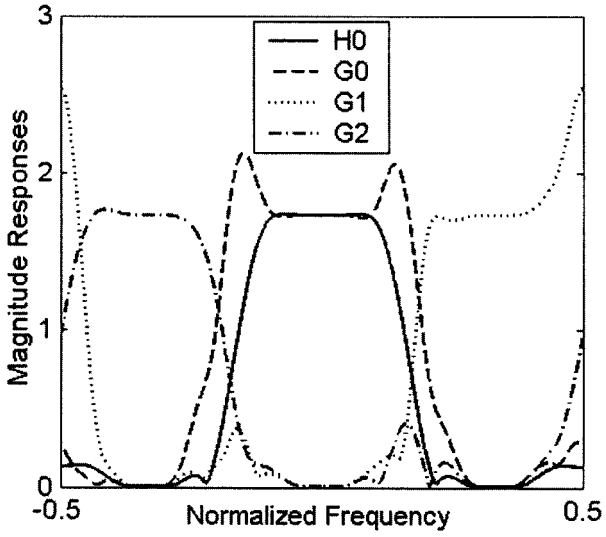

Fig. 8. Optimized type I filterbank with $L=7$ and $K=4$.

exponent 2.9192, and the total stopband energy of three analysis filters is 0.0877. From the two examples, the type II lifting scheme seems to outperform the type I lifting scheme, as it generates real and symmetric dual scaling filters and filterbanks with lower stopband sidelobes.

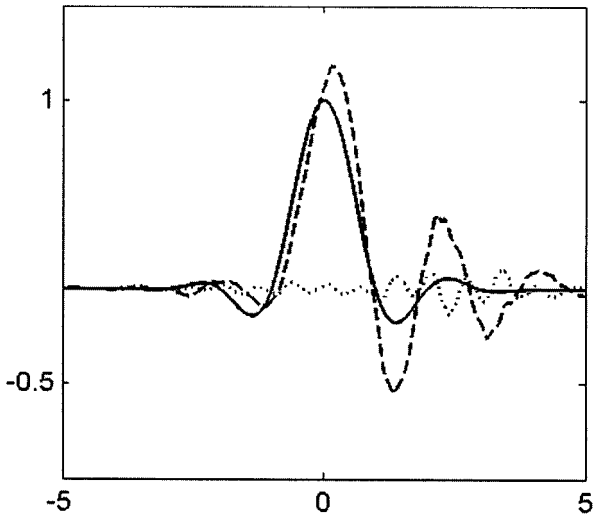

Fig. 9. Scaling function and its dual for the filterbank in Fig. 8.

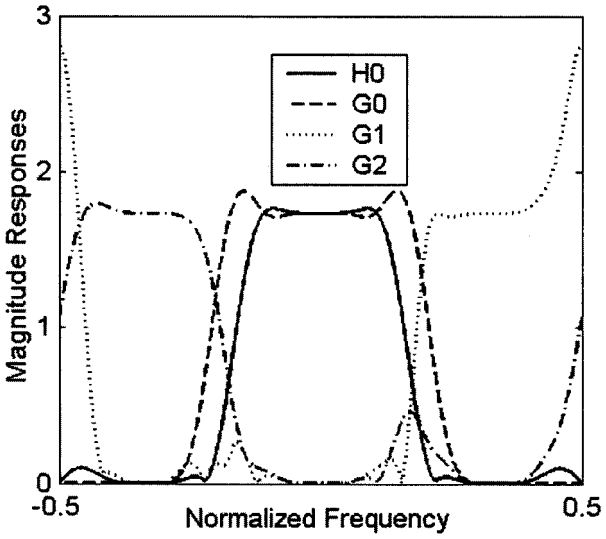

Fig. 10. Optimized type II filterbank with $L = 7$ and $K = 4$.

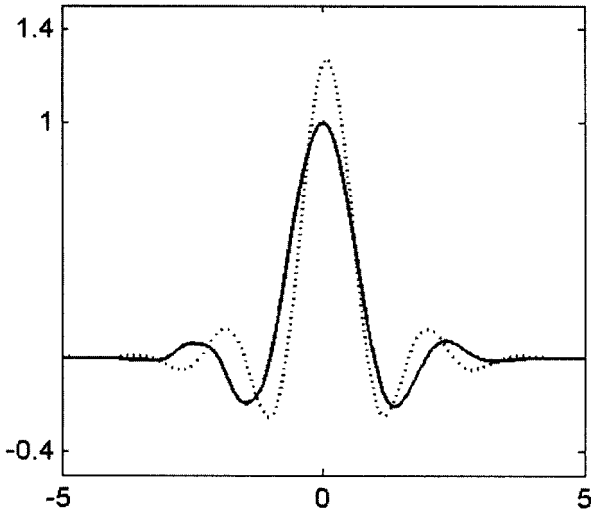

Fig. 11. Scaling function and its dual for the filterbank in Fig. 10.

V. Conclusion

In this paper, we give the two types of three-band lifting schemes, from which two families of three-band interpolating complex filterbanks and wavelets are devised. Unlike the traditional two-band complex filterbanks and wavelets, novel three-band complex filterbanks are composed of three channels: the lowpass channel, the positive highpass channel, and the negative highpass channel. They provide the ability to partition positive and negative components in complex signals into different subbands/channels, which is very attractive in some applications. Moreover, the stopband suppression are used to handle the stopband attenuation and the passband flatness of highpass filters. Two elegant theorems are proved, and the numerical method may be employed to further lower the stopband sidelobes and improves smoothness of scaling functions. Utilizing these results, we can construct interpolating complex filterbanks with arbitrary order regularity and stopband suppression.

However, we also notice that negative frequency components may leak into the positive frequency channel and vice versa. This is an inherent deficiency of three-band complex filterbanks. For FIR complex filterbanks, the positive highpass filters H_1 and G_1 cannot sharply attenuate to zero at the right side of $\omega = \pi$, and thus, its transition band cannot but extend into the negative frequency region. In order to overcome this deficiency, we may consider M-band ($M > 3$) complex filterbanks via the M-band lifting scheme. For example, in the four-band case, the ideal complex filterbank includes four channels: the lowpass channel, the positive bandpass channel, the negative bandpass channel, and the highpass channel. In this case, for the two bandpass channels, this phenomena should be avoided. In the future, we will extend this design method to the general M-band case.

Appendix A
Proof of Theorem 1

Proof: We first prove that when the filterbank $\{H_0, H_1, H_2\}$ is $(K+1)$-regular and of $(K+1)$-order stopband suppression, the lifting filters satisfy the moment condition (16). Below, we frequently utilize the relations $\alpha^3 = \alpha^{-3} = 1$, $\alpha^{-1} = \alpha^2$ and $\overline{\alpha} = \alpha^2$ for the complex number $\alpha = e^{j(2/3)\pi}$.

From (9)

$$H_0(\omega) = 1 + e^{-j\omega}T_{01}(e^{3j\omega}) + e^{-2j\omega}T_{01}(e^{3j\omega})$$

where $H_0(2\pi/3) = H_0(-(2\pi/3)) = 0$ is equivalent to

$$1 + \alpha^{-1}v_{01}(0) + \alpha v_{02}(0) = 0$$
$$1 + \alpha v_{01}(0) + \alpha^{-1}v_{02}(0) = 0.$$

We obtain

$$v_{01}(0) = v_{02}(0) = 1. \tag{26}$$

For $k \geqslant 1$ and $q = 0, \pm 1$

$$H_0^{(k)}\left(\frac{2\pi}{3}q\right) = (-3j)^k \alpha^{-q} \sum_{p=0}^{k} \cdot C_k^p \left[\left(\tfrac{1}{3}\right)^p v_{01}(k-p) + \alpha^{-2q}\left(\tfrac{2}{3}\right) v_{02}(k-p)\right]. \tag{27}$$

From $H_0^{(k)}(\pm(2/3)\pi)=0$, for $k=1,\ldots,K$, we derive

$$\begin{bmatrix}1 & \alpha^{-1}\\ 1 & \alpha\end{bmatrix}\begin{bmatrix}\sum_{p=0}^{k}(-j)^k C_k^p\left(\frac{1}{3}\right)^p v_{01}(k-p)\\ \sum_{p=0}^{k} C_k^p\left(\frac{2}{3}\right)^p v_{02}(k-p)\end{bmatrix}=\begin{bmatrix}0\\0\end{bmatrix}. \quad (28)$$

The coefficient matrix in (28) is nonsingular, and thus, this homogeneous system of linear equations only has a trivial solution, that is, for $k=1,\ldots,K$

$$\sum_{p=0}^{k} C_k^p\left(\tfrac{1}{3}\right)^p v_{01}(k-p)=0$$
$$\sum_{p=0}^{k} C_k^p\left(\tfrac{2}{3}\right)^p v_{02}(k-p)=0. \quad (29)$$

Combining (26) and (29), we obtain, for $k=0,1,\ldots,K$

$$v_{01}(k)=\left(-\tfrac{1}{3}\right)^k,\qquad v_{01}(k)=\left(-\tfrac{2}{3}\right)^k. \quad (30)$$

Moreover, when (30) holds, for $k=0,1,\ldots,K$

$$H_0^{(k)}(0)=3\delta(k).$$

Further, $H_1(\omega)$ is of $(K+1)$-order stopband suppression, that is

$$H_1^{(k)}(0)=(-3j)^k\left[\left(\tfrac{1}{3}\right)^k+3v_{10}(k)+\sum_{p=0}^{k}C_k^p\left(\tfrac{2}{3}\right)^p v_{12}(k-p)\right]=0$$
$$H_1^{(k)}\left(-\tfrac{2}{3}\pi\right)=(-3j)^k\alpha\left[\left(\tfrac{1}{3}\right)^k+\alpha\sum_{p=0}^{k}C_k^p\left(\tfrac{2}{3}\right)^p v_{12}(k-p)\right]=0. \quad (31)$$

From (31), we obtain

$$v_{10}(k)=\frac{\alpha^2-1}{3}\left(\frac{1}{3}\right)^k,\quad v_{12}(k)=-\alpha^2\left(-\frac{1}{3}\right)^k. \quad (32)$$

Moreover, when (30) and (32) hold

$$H_1^{(k)}\left(\tfrac{2}{3}\pi\right)=(-j)^k(\alpha^2-1).$$

Similarly, from $H_2^{(k)}(0)=H_2^{(k)}((2/3)\pi)=0$, for $k=0,1,\ldots,K$, i.e.,

$$H_2^{(k)}(0)=(-2j)^k+3(-3j)^k v_{20}(k)=0$$
$$H_2^{(k)}\left(\tfrac{2}{3}\pi\right)=(-2j)^k\alpha^{-2}+(\alpha^2-1)(-3j)^k\sum_{p=0}^{k}\cdot C_k^p v_{21}(p)\left(\tfrac{1}{3}\right)^{k-p}=0 \quad (33)$$

we obtain

$$v_{20}(k)=-\frac{1}{3}\left(\frac{2}{3}\right)^k,\qquad v_{21}(k)=\frac{\alpha}{1-\alpha^2}\left(\frac{1}{3}\right)^k$$
$$H_2^{(k)}\left(-\tfrac{2}{3}\pi\right)=(-2j)^k\alpha^2.$$

Contrarily, when the lifting filters satisfy the moment condition (16), it is easy to verify that the scaling filter H_0 is $(K+1)$-regular and that the two highpass filters H_1 and H_2 have $(K+1)$-order stopband suppression. The first part of Theorem 1 is proved.

Further, from (10), we have

$$G_2(\omega)=e^{-2j\omega}-\overline{T}_{02}(e^{-3j\omega})+\overline{T}_{12}(e^{-3j\omega})\overline{T}_{01}(e^{-3j\omega})-e^{-j\omega}\overline{T}_{12}(e^{-3j\omega}). \quad (34)$$

When (16) is satisfied, for $q=0$ and ±1, we have

$$G_2^{(k)}\left(\frac{2\pi}{3}q\right)=(-2j)^k\alpha^{-2q}-(3j)^k\overline{v}_{02}(k)+\sum_{p=0}^{k}\cdot C_k^p\left[(3j)^k\overline{v}_{12}(p)\overline{v}_{01}(k-p)-(-j)^p\alpha^{-q}(3j)^{k-p}\overline{v}_{12}(k-p)\right]$$
$$=(-2j)^k\alpha^{-2q}-(-2j)^k+\sum\cdot C_k^p(-j)^k\left[\left(-\overline{\alpha^2}\right)+\alpha^{-q}\overline{\alpha^2}\right]\left(\text{note: }\overline{\alpha^2}=\alpha\right)$$
$$=(-2j)^k[\alpha^{-2q}-1-\alpha+\alpha^{-q}\alpha].$$

Obviously

$$G_2^{(k)}(0)=(-2j)^k[1-1-\alpha+\alpha]=0$$
$$G_2^{(k)}\left(\tfrac{2}{3}\pi\right)=(-2j)^k[\alpha^{-2}-1-\alpha+\alpha^{-1}\alpha]=0$$
$$G_2^{(k)}\left(-\tfrac{2}{3}\pi\right)=(-2j)^k[2\alpha^2-\alpha-1]=3\alpha^2(-2j)^k\ (\text{note: }1+\alpha+\alpha^2=0). \quad (35)$$

Similarly

$$G_1^{(k)}\left(\frac{2\pi}{3}q\right)=(-j)^k\alpha^{-q}-(-j)^k-\sum_{p=0}^{k}C_k^p(3j)^p\cdot\left(\frac{1}{3}\right)^p\frac{\overline{\alpha}}{1-\overline{\alpha^2}}(-2j)^{k-p}3\alpha^2\delta(q+1)$$
$$=(-j)^k\left[\alpha^{-q}-1-\delta(q+1)\frac{3\alpha}{1-\alpha}\right]\left(\text{note: }\overline{\alpha}=\alpha^2,\ \overline{\alpha^2}=\alpha\right)$$
$$=(-j)^k[\alpha^{-q}-1-\delta(q+1)(\alpha-1)].$$

Therefore, for $k=0,1,\ldots,K$

$$G_1^{(k)}\left(\frac{2\pi}{3}\right)=(-j)^k(\alpha^2-1)$$
$$G_1^{(k)}(0)=0,\qquad G_1^{(k)}\left(-\frac{2\pi}{3}\right)=0.$$

Using the similar method, we can prove the following: For $k=0,1,\ldots,K$

$$G_0^{(k)}\left(\pm\frac{2\pi}{3}\right)=0,\qquad G_0^{(k)}(0)=\delta(k).$$

Therefore, the dual scaling filter is $(K+1)$-regular, and the two dual highpass filters have $(K+1)$-order stopband suppression. Theorem 1 is completed. ■

Appendix B
Proof of Theorem 2

Since the scaling filter $H_0(\omega)$ in the type II is identical with that in the type I, Theorem 1 has shown that when $H_0(\omega)$ is $(K+1)$-regular, the lifting filters t_{01} and t_{02} must satisfy the following: For $k=0,1,\ldots,K$

$$v_{01}(k)=\left(-\tfrac{1}{3}\right)^k,\qquad v_{01}(k)=\left(-\tfrac{2}{3}\right)^k \quad (36)$$

and for $k = 0, 1, \ldots, K$

$$H_0^{(k)}(0) = 3\delta(k). \tag{37}$$

When $H_1(\omega)$ in (11) has $(K+1)$-order stopband suppression, $H_0^{(k)}(-(2/3)\pi) = 0$ for $k = 0, 1, \ldots, K$, and thus

$$H_1^{(k)}\left(-\tfrac{2}{3}\pi\right) = (-j)^k\alpha + (-3j)^k\alpha^2 \sum_{p=0}^{k} C_k^p v_{12}(p)\left(\tfrac{2}{3}\right)^{k-p} = 0. \tag{38}$$

Therefore, for $k = 0, 1, \ldots, K$

$$v_{12}(k) = -\alpha^2\left(-\tfrac{1}{3}\right)^k. \tag{39}$$

Further, utilizing (39) and $H_0^{(k)}(0) = 3\delta(k)$ and $H_0^{(k)}((2/3)\pi) = 0$ for $k = 0, 1, \ldots, K$, we obtain

$$\begin{aligned} H_1^{(k)}(0) &= (-j)^k(1-\alpha^2) + 3(-3j)^k \\ &\quad \cdot \left[v_{10}(k) - \alpha^2 \sum_{p=0}^{k} C_k^p v_{20}(p)\left(-\tfrac{1}{3}\right)^{k-p}\right] = 0 \\ H_1^{(k)}\left(\tfrac{2}{3}\pi\right) &= (-j)^k\alpha^{-1} + \alpha^{-2}\alpha^2 \sum_{p=0}^{k} \\ &\quad \cdot C_k^p(-2j)^p(-3j)^{k-p}\left(-\tfrac{1}{3}\right)^{k-p} \end{aligned}$$

that is

$$\begin{aligned} v_{10}(k) - \alpha^2 \sum_{p=0}^{k} C_p^k v_{20}(p)\left(-\frac{1}{3}\right)^{k-p} &= \frac{\alpha^2-1}{3^{k+1}} \\ H_1^{(k)}\left(\tfrac{2}{3}\pi\right) = (-j)^k(\alpha^{-1}-1) &= (-j)^k(\alpha^2-1). \end{aligned} \tag{40}$$

Since $H_2(\omega)$ in (11) has $(K+1)$-order stopband suppression, we have for $k = 0, 1, \ldots, K$

$$\begin{aligned} H_2^{(k)}(0) &= (-2j)^k + 3(-3j)^k v_{20}(k) = 0 \\ H_2^{(k)}\left(\tfrac{2}{3}\pi\right) &= (-2j)^k\alpha^{-2} + (-3j)^k(\alpha^{-1}-1)\sum_{p=0}^{k} \\ &\quad \cdot C_p^k v_{21}(p)\left(\tfrac{1}{3}\right)^{k-p} = 0 \\ H_2^{(k)}\left(-\tfrac{2}{3}\pi\right) &= (-2j)^k\alpha^2. \end{aligned}$$

Therefore

$$\begin{aligned} v_{20}(k) &= -\tfrac{1}{3}\left(\tfrac{2}{3}\right)^k \\ v_{21}(k) &= \frac{\alpha}{1-\alpha^2}\left(\tfrac{2}{3}\right)^k. \end{aligned} \tag{41}$$

Substitute the first equation in (41) into the second equation in (40) and then obtain

$$v_{10}(k) = -\frac{1}{3^{k+1}}. \tag{42}$$

Contrarily, when the lifting filters satisfy the moment condition (17), it is easy to verify that the scaling filter H_0 is $(K+1)$-regular and that the two highpass filters H_1 and H_2 have $(K+1)$-order stopband suppression. Further, since G_1 and G_2 in the type II are identical with those in the type I and in (16) and (17), t_{01}, t_{02}, t_{12} and t_{21} satisfy the same moment conditions. From the proof of Theorem 1, we know G_1 and G_2 have $(K+1)$ order stopband suppression. In what follows, we verify that G_0 is $(K+1)$-regular. When $k = 0$

$$\begin{aligned} G_0(0) &= 1 \\ G_0\left(\frac{2}{3}\pi\right) &= \frac{1+\alpha^{-1}+\alpha^{-2}}{3} = 0 \\ G_0\left(-\frac{2}{3}\pi\right) &= \frac{1+\alpha+\alpha^2}{3} = 0. \end{aligned}$$

For $k = 1, 2, \ldots, K$, it is easy to verify that

$$G_0^{(k)}\left(\frac{2q}{3}\pi\right) = 0, \qquad \text{for } q = 0 \text{ and } \pm 1.$$

The proof of Theorem 2 is finished. ■

Appendix C
Proof of Corollary 1

Property (16) has been proved in Theorems 1 and 2, which show that two scaling filters are at least $2(K+1)$-order flat.

In fact, from the proofs of Theorems 1 and 2, we have observed that

$$\begin{aligned} H_1^{(k)}\left(\frac{2\pi}{3}\right) &= G_1^{(k)}\left(\frac{2\pi}{3}\right) = (-j)^k(\alpha^2-1) \\ 3H_2^{(k)}\left(-\frac{2\pi}{3}\right) &= G_1^{(k)}\left(-\frac{2\pi}{3}\right) = 3\alpha^2(-2j)^k. \end{aligned}$$

For $k = 1, 2, \ldots, K$, we have

$$\begin{aligned} \left.\frac{d^{(k)}|H_1(\omega)|^2}{d\omega^k}\right|_{\omega=2\pi/3} &= \left.\frac{d^{(k)}(H_1(\omega)\tilde{H}_1(\omega)}{d\omega^k}\right|_{\omega=2\pi/3} \\ &= \sum_{p=0}^{k} C_k^p H_1^{(p)}\left(\frac{2\pi}{3}\right)\tilde{H}_1^{(k-p)}\left(\frac{2\pi}{3}\right) \\ &= |\alpha^2-1|^2 \sum_{p=0}^{k} C_p^k(-j)^p j^{k-p} = 0 \end{aligned}$$

where $\tilde{H}_1(\omega)$ is the conjugate of $H_1(\omega)$. Therefore, $H_1(\omega)$ is $(K+1)$-order flat around $\omega = 2\pi/3$. Similarly, we can prove that H_2, G_1 and G_2 are $(K+1)$-order flat around the centers of their passbands. ■

Appendix D
Proof of Proposition 1

From (24), when $K = 2K_1$ is an even integer, then

$$\begin{aligned} m_{01} &= [-K_1 - 1/3] = -K_1 \\ m_{02} &= [-K_1 - 2/3] = -K_1 - 1. \end{aligned}$$

According to (22)

$$\begin{aligned} t_{02}(n) &= \prod_{k=-K_1-1,\, k\neq n}^{K_1-1} \frac{3k+2}{3(k-n)} \\ &\overset{k'=-(k+1)}{=} \prod_{k'=K_1,\, k'\neq -(n+1)}^{-K_1} \frac{3k'+1}{3(k'+n+1)} = t_{01}(-n-1). \end{aligned}$$

Therefore

$$T_{02}(z) = \sum_{n=-K_1-1}^{K_1-1} t_{02}(n)z^{-n} \overset{n'=-(n+1)}{=} \sum_{n=K_1}^{-K_1} t_{01}(n')z^{n'+1} = zT_{01}(z^{-1}).$$

When $K = 2K_1 - 1$ is an odd integer $m_{01} = m_{02} = -K_1$, by the similar method, we can prove that

$$T_{02}(z) = zT_{01}(z^{-1}). \tag{43}$$

From this equation, we obtain

$$\begin{aligned} H_0(z) &= 1 + z^{-1}T_{01}(z^3) + z^{-2}T_{02}(z^3) \\ &= 1 + z^{-1}T_{01}(z^3) + zT_{01}(z^{-3}) \end{aligned}$$

that is, $H_0(z^{-1}) = H_0(z)$, and thus, H_0 is symmetric.

Additionally

$$H(z) = 1 + \sum_{n=m01}^{m01+K} t_{01}(n)z^{-(3n+1)} + \sum_{n=m02}^{m02+K} t_{02}(n)z^{-(3n+2)}$$

and thus, the length of H_0 satisfies

$$\begin{aligned} Length(H_0) &= \max\{3K + 3m_{01} + 1,\, 3K + 3m_{02} + 2\} \\ &\quad - \min\{3m_{01} + 1,\, 3m_{02} + 2\} + 1 \\ &= \max\{3K,\, 3K + 3(m_{01} - m_{02}) - 1 \\ &\qquad 3K - 3(m_{01} - m_{02}) + 1\} + 1 \\ &= 3K + 1 + |3(m_{01} - m_{02}) - 1|. \end{aligned} \tag{44}$$

When K is an odd integer, $m_{01} = m_{02}$, and H_0 achieves the shortest length $3K + 2$. When K is an even integer, due to symmetry, $Length(H_0)$ must be an odd integer, and $m_{01} - m_{02} = 1$ makes $Length(H_0)$ be minimal and equal to $3K + 3$. Consequently, the (24) generates the symmetric interpolating scaling filter H_0 with the shortest length.

For the type II filterbank, from $m_{10} = [-(K/2) + (1/3)]$, $m_{20} = [-(K/2) + (2/3)]$, and (22), we can obtain

$$T_{20}(z) = z^{-1}T_{10}(z^{-1}). \tag{45}$$

Using (43) and (45), it is easy to verify that $G_0(z^{-1}) = G_0(z)$, and thus, G_0 is also symmetric. ■

ACKNOWLEDGMENT

The authors would like to thank the reviewers for their insightful comments, which greatly improved the quality of this paper.

REFERENCES

[1] I. Daubechies, "Orthonormal bases of compactly supported wavelets," *Commun. Pure Appl. Math.*, vol. 41, pp. 909–996, 1988.

[2] C. K. Chui and J. Z. Wang, "A general framework of compactly supported splines and wavelets," *J. Approx. Theory*, vol. 71, no. 3, pp. 263–304, 1992.

[3] A. Cohen, I. Daubechies, and J. Feauveau, "Biorthogonal bases of compactly supported wavelets," *Commun. Pure Appl. Math.*, vol. 45, pp. 485–560, 1992.

[4] M. Vetterli and C. Herley, "Wavelets and filter banks: Theory and design," *IEEE Trans. Signal Processing*, vol. 40, pp. 2207–2232, Sept. 1992.

[5] M. Unser, P. Thévenaz, and A. Aldroubi, "Shift-orthogonal wavelet bases," *IEEE Trans. Signal Processing*, vol. 46, pp. 1827–1836, July 1998.

[6] A. K. Soman, P. P. Vaidyanathan, and T. Q. Nguyen, "Linear phase paraunitary filterbanks: Theory, factorization and designs," *IEEE Trans. Signal Processing*, vol. 41, pp. 3480–3496, Dec. 1993.

[7] P. Steffen, P. N. Heller, R. A. Gopinath, and C. S. Burrus, "Theory of regular M-band wavelet bases," *IEEE Trans. Signal Processing*, vol. 41, pp. 3497–3510, Dec. 1993.

[8] J. Lebrun and M. Vetterli, "High-order balanced multiwavelets: Theory, factorization, and design," *IEEE Trans. Signal Processing*, vol. 49, pp. 1918–1930, Sept. 2001.

[9] D. C. Schleher, *MTI and Pulse Doppler Radar*. Norwood, MA: Artech House, 1991.

[10] L. G. Weiss, "Wavelets and wideband correlation processing," *IEEE Signal Processing Mag.*, vol. 11, pp. 13–32, Jan. 1994.

[11] L. Cohen, "Time-frequency distribution—A review," *Proc. IEEE*, vol. 77, pp. 941–981, July 1989.

[12] I. Daubechies, "The wavelet transform, time-frequency localization and signal analysis," *IEEE Trans. Inform. Theory*, vol. 36, pp. 961–1005, Apr. 1990.

[13] S. Mann and S. Haykin, "Time-frequency perspectives: The chirplet transform," in *Proc. IEEE ICASSP*, vol. 3, 1992, pp. 417–420.

[14] S. G. Mallat and Z. Zhang, "Matching pursuits with time-frequency dictionaries," *IEEE Trans. Signal Processing*, vol. 41, pp. 3397–3415, Dec. 1993.

[15] W. Lawton, "Applications of complex valued wavelet transform to subband decomposition," *IEEE Trans. Signal Processing*, vol. 41, pp. 3566–3568, Dec. 1993.

[16] X. P. Zhang, M. Desai, and Y. N. Peng, "Orthogonal complex filterbanks and wavelets: Some properties and design," *IEEE Trans. Signal Processing*, vol. 47, pp. 1039–1048, Apr. 1999.

[17] X. Q. Gao, T. Q. Nguyen, and G. Strang, "Theory and lattice structure of complex paraunitary filterbanks with filters of (Hermitian-) symmetry/antisymmetry properties," *IEEE Trans. Signal Processing*, vol. 49, pp. 1028–1043, May 2001.

[18] J. M. Lina and M. Mayrand, "Complex Daubechies wavelets," *Appl. Comput. Harmon. Anal.*, vol. 2, no. 3, pp. 219–229, 1995.

[19] X. Q. Gao, T. Q. Nguyen, and G. Strang, "A study of two-channel complex-valued filterbanks and wavelets with orthogonality and symmetry properties," *IEEE Trans. Signal Processing*, vol. 50, pp. 824–833, Apr. 2002.

[20] J. Magarey and N. Kingsbury, "Motion estimation using a complex-valued wavelet transform," *IEEE Trans. Signal Processing*, vol. 46, pp. 1069–1084, Apr. 1998.

[21] H. Malvar, "A modulated complex lapped transform and its applications to audio processing," in *Proc. ICASSP*, vol. 3, 1999, pp. 1421–1424.

[22] N. Kingsbury, "Complex wavelets for shift invariant analysis and filtering of signal," *Appl. Harmon. Anal.*, vol. 10, no. 3, pp. 234–253, May 2001.

[23] I. W. Selesnick, "Hilbert transform pair of wavelet bases," *IEEE Trans. Signal Processing Lett.*, vol. 8, pp. 170–173, June 2001.

[24] ——, "The design of Hilbert transform pair of wavelet bases," *IEEE Trans. Signal Processing*, vol. 50, pp. 1144–1152, May 2002.

[25] F. C. A. Fernandes, F. C. A. s, R. Van. Spaendonck, and C. S. Burrus, "A new directional, low-redundancy, complex-wavelet transform," in *Proc. ICASSP*, pp. 3653–3656.

[26] F. C. A. Fernandes, "Directional, shift-insensitive complex wavelet transforms with controllable redundancy," Ph.D. dissertation, Rice Univ., Houston, TX [Online]. Available: http://www.ece.rice.edu/felixf/dissertation.pdf, Jan. 2002.

[27] W. Sweldens, "The lifting scheme: A construction of second generation wavelets," *SIAM J. Math. Anal.*, vol. 29, no. 2, pp. 511–546, Mar. 1997.

[28] ——, "The lifting scheme: A custom-design construction of biorthogonal wavelets," *Appl. Comput. Harmon. Anal.*, vol. 3, no. 2, pp. 186–200, Mar. 1996.

[29] I. Daubechies and W. Sweldens, "Factoring wavelet transforms in lifting steps," *J. Fourier Anal. Appl.*, vol. 4, no. 3, pp. 245–267, 1998.

[30] Lounsbery, T. D. DeRose, and J. Warren, "Multiresolution analysis for surfaces of arbitrary topological type," *ACM Trans. Graph.*, vol. 16, no. 1, pp. 34–73, 1997.

[31] A. Harten, "Multiresolution representation of data: A general framework," *SIAM J. Numer. Anal.*, vol. 33, no. 3, pp. 1205–1256, 1996.

[32] J. Kovavčević and W. Sweldens, "Wavelet families of increasing order in arbitrary dimensions," *IEEE Trans. Image Processing*, vol. 9, pp. 480–496, Mar. 2000.

[33] P. P. Vaidyanathan and A. Kiraç, "Result on optimal biorthogonal filter banks," *IEEE Trans. Circuits Syst. II*, vol. 45, pp. 932–947, Aug. 1998.
[34] N. V. Boulgouris, D. Tzovaras, and M. G. Strintzis, "Lossless image compression based on optimal prediction, adaptive lifting, and conditional arithmetic coding," *IEEE Trans. Image Processing*, vol. 10, pp. 1–14, Jan. 2001.
[35] P.-L. Shui and Z. Bao, "Recursive biorthogonal interpolating wavelets and signal-adapted interpolating filter banks," *IEEE Trans. Signal Processing*, vol. 47, pp. 2585–2594, Sept. 2000.
[36] X.-G. Xia and Z. Zheng, "On sampling theorem, wavelets, and wavelet transforms," *IEEE Trans. Signal Processing*, vol. 41, pp. 3524–3535, Feb. 1993.
[37] D. L. Donoho, *Interpolating Wavelet Transforms*. Stanford, CA: Preprint, Dept. Statist., Stanford Univ., 1992.
[38] P.-L. Shui, Z. Bao, and X.-D. Zhang, "M-band compactly supported orthogonal symmetric interpolating scaling functions," *IEEE Trans. Signal Processing*, vol. 49, pp. 1704–1713, Aug. 2001.
[39] R. L. De Queiroz and K. R. Rao, "Time-frequency lapped transforms and wavelets packets," *IEEE Trans. Signal Processing*, vol. 41, pp. 3293–3305, Dec. 1993.
[40] S. Dubuc, "Interpolation through an iterative scheme," *J. Math. Anal. Appl.*, vol. 144, pp. 185–204, 1986.
[41] H. Ji and Z. Shen, "Compactly supported (bi)orthogonal wavelets generated by interpolatory refinable functions," *Adv. Comput. Math.*, vol. 11, pp. 81–104, 1999.

Peng-Lang Shui (M'99) received the M.S. degree in mathematics from Nanjing University, Nanjing, China, and the Ph.D. degree in signal and information processing from Xidian University, Xi'an, China, in 1992 and 1999, respectively.

He is now a Professor with the Department of Applied Mathematics and Key Laboratory for Radar Signal Processing, Xidian University. His research interest includes digital signal processing, wavelets and multirate filterbanks, data compression, and ultra wideband radar signal processing.

Zheng Bao (M'80–SM'90) received the B.S. degree in the radar engineering from Xidian University, Xi'an, China.

He is now a Professor at Xidian University. He has been working in a number of areas, including radar systems, signal processing, neural networks, and automatic target recognition. He has published more than 200 journal papers and is the author or coauthor of ten books. His current research interest includes radar signal processing, array signal processing, and SAR/ISAR imaging.

Prof. Bao is a member of the Chinese Academy of Sciences.

Yuan Yan Tang (SM'96) received the B.S. degree in electrical and computer engineering from Chongqing University, Chongqing, China, the M.Eng. degree in electrical engineering from the Graduate School of Post and Telecommunications, Beijing, China, and the Ph.D. degree in computer science from Concordia University, Montreal, QC, Canada.

He is presently a Professor with the Department of Computer Science, Hong Kong Baptist University, and Adjunct Professor of computer science at Concordia University. He is an Honorary Lecturer at the University of Hong Kong and an Advisory Professor at many institutes in China. His current interests include wavelet theory and applications, pattern recognition, image processing, document processing, artificial intelligence, parallel processing, Chinese computing, and VLSI architecture. He has published more than 200 technical papers and is the author/coauthor of 18 books on subjects ranging from electrical engineering to computer science. He is the Founder and Editor-in-Chief of the *International Journal on Wavelets, Multiresolution, and Information Processing (IJWMIP)* and is an Associate Editor of several international journals.

Prof. Tang has served as General Chair, Program Chair, and Committee Member for many international conferences.